BIODIVERSITAS
Volume 23, Number 8, August 2022
Pages: 4097-4108

ISSN: 1412-033X
E-ISSN: 2085-4722
DOI: 10.13057/biodiv/d230830

Morpho-anatomical characterization and DNA barcode of *Cosmos caudatus* Kunth.

HERY PURNOBASUKI[1,2,♥], GALUH AYU RAKHASHIWI[1], JUNAIRIAH[1], DWI KUSUMA WAHYUNI[1,2], RAMADHANI EKA PUTRA[3], RIKA RAFFIUDIN[4], RC HIDAYAT SOESSILOHADI[5]

[1]Department of Biology, Faculty of Science and Technology, Universitas Airlangga. Jl. Dr. Ir. H. Soekarno, Surabaya 60115, East Java, Indonesia. Tel.: +62-31-5936501, Fax.: +62-31-5936502. ♥email: hery-p@fst.unair.ac.id
[2]Biotechnology of Tropical Medicinal Plants Research Group, Universitas Airlangga. Jl. Dr. Ir. H. Soekarno, Surabaya 60115, East Java, Indonesia
[3]School of Life Sciences and Technology, Institut Teknologi Bandung. Jl. Ganeca No.10, Bandung 40132, West Java, Indonesia
[4]Department of Biology, Faculty of Mathematic and Natural Sciences, Institut Pertanian Bogor. Jl. Meranti, Kampus IPB Darmaga, Bogor 16680, West Java, Indonesia
[5]Faculty of Biology, Universitas Gadjah Mada. Jl. Teknika Selatan, Sleman 55281, Yogyakarta, Indonesia

Manuscript received: 24 March 2022. Revision accepted: 26 July 2022.

Abstract. *Purnobasuki H, Rakhashiwi GA, Junairiah, Wahyuni DK, Putra RE, Raffiudin R, Soessilohadi RCH. 2022. Morpho-anatomical characterization and DNA barcode of* Cosmos caudatus *Kunth. Biodiversitas 23: 4097-4108.* Secondary metabolites in plants have various benefits, therefore their distribution in plant body parts is important to study. The identification process of plants should be conducted using several characters, including morphological and molecular data. This study aimed to identify and confirm *Cosmos caudatus* Kunth using morpho-anatomy characters and DNA barcodes. The plants used were three samples taken from the Husada Graha Famili Park, Surabaya. The morpho-anatomical investigation was carried out descriptively, while the DNA barcoding study was processed by amplifying and sequencing the *rbcL* and *matK* genes. Morphological studies indicate that the roots and stems of *C. caudatus* are similar to the organs of dicots shrubs in general. The leaves have a pinnate type with two different colors on each side of the leaf. Compound flowers are cup-type with two types of flowers, namely disc flowers and ray flowers. Based on anatomical observation, all vegetative organs have the same tissue as dicotyledonous plants. The anatomical characteristic of *C. caudatus* lies in its trichomes due to its anthocyanin content and stomata which are anomocytic and anisocytic types. DNA barcoding results showed that the three sample plants had identical similarities with several *Cosmos* genera contained in the GenBank database with percentage identities values above 98%, query covers 96-100%, and e-values of 0.

Keywords: Barcode, *Cosmos caudatus*, *matK*, genetic diversity, morpho-anatomy, *rbcL*

Abbreviations: DNA: Deoxyribonucleic acid, *matK: maturase-K, rbcL: ribulose-bisphosphate carboxylase large* subunit, CBOL: Consortium for Barcode of Life, PCR: Polymerase chain reaction, BLAST: Basic Local Alignment Search Tool

INTRODUCTION

Cosmos caudatus Kunth has known locally as Kenikir, belongs to the family Asteraceae (Cheng et al. 2015; Yusoff et al. 2021). The family is distributed throughout Neotropics (POWO 2022) and often makes up the forest floor vegetation, including *C. caudatus* (Christenhusz and Byng 2016; Panero and Crozier 2016; Willis 2017). The species is herbal plant originating from Latin America and then spreading to Southeast Asia (Bodeker 2009; Moshawih et al. 2017).

Cosmos caudatus has abundant benefits, including antibacterial (Yusoff et al. 2014; Safita et al. 2015), anti-inflammatory (Ajaykumar et al. 2012), antioxidant and anticancer (Cheng et al. 2015). Various health benefits of the species are due to the presence of secondary metabolites (Mediani et al. 2013). According to Moshawih et al. (2017), *C. caudatus* has various secondary metabolites, including flavonoids, saponins, terpenoids, tannins, and phenols. The presence of bioactive components can be found by analyzing plant extracts, especially on the leaves (Phong et al. 2022). Wahyuni et al. (2019) add that secondary metabolites can be found in specific areas of plant organs. To comprehend the location of cells that store the secondary metabolites, anatomical research is necessary (Ilham et al. 2022), since anatomical characteristics can also help identify plants. Therefore, its values are crucial for classifying plants. Rahman et al. (2013) reported anatomical features of 36 plant species from the Rajshahi division, Bangladesh, including *C. caudatus*. The species has stomata with anomocytic and anisocytic types.

Classification and phylogenetic studies mainly depend on morphological cues (Kaur and Singh 2020). The weakness of morphological markers is in terms of variability, and it can cause serious taxonomic problems in species with a wide geographic range. Abiotic factors can substantially impact both micro and macromorphological features, even though ontogenetic programming contributes to morphological variability in some cases. As an example, *Cosmos bipinnatus* in Central Mexico exhibits intricate morphological variations due to environmental conditions, such as height and NH_4 content surrounding the plant's habitat (Paniagua-Ibánez et al. 2015).

The lack of morphological data can be supplemented in several ways, including by using additional identification markers like DNA barcoding and anatomical features. DNA barcoding is a technique for identifying species by examining short sequences of the standard genome and comparing the results with a database of known species (Yu et al. 2021). One of the specific purposes of DNA barcoding is to confirm the therapeutic plant content in herbal products (Chen et al. 2014; de Boer et al. 2015). Several recommended plastid markers in plants include *rpoC1*, *rpoB*, *trnH-psbA*, *rbcL*, *matK*, *atpF-H*, and *psbK-I* (Hollingsworth et al. 2011). Of which, *rbcL* and *matK* are suggested for DNA barcoding by the Consortium Barcode of Life Plant Working Group (CBOL) (Michel et al. 2016).

Plant identification should be conducted using several characters, including morphological and molecular data to avoid ambiguous understanding, mainly when studying plant biological systems in pharmaceutical aspects (Wahyuni et al. 2019; Ilham et al. 2022). This study aimed to confirm and identify *C. caudatus* using morpho-anatomy and DNA barcoding. The results of this study should attest to the veracity of these plant species, and the data can be used to help the pharmaceutical industry, in particular in the field of herbal medicines and green products to support life, in ascertaining the kinds of herbal medicinal substances.

MATERIALS AND METHODS

Plant materials

Mature plant samples of *Cosmos caudatus* were collected in September 2019 at Taman Husada Graha Famili, Surabaya, East Java, Indonesia. Plant samples were taken from as many as three individuals. Species identification has been confirmed by comparing it with the herbarium collection in the Purwodadi Botanical Garden, Indonesian Institute of Sciences, Pasuruan, East Java, Indonesia.

Morpho-anatomy observation

All plant parts were thoroughly examined as part of morphological research, commencing with the roots, stems, leaves, flowers, fruits, and seeds. Anatomical research is restricted to vegetative organs, such as the roots, stems, and leaves. The paraffin method was used to prepare anatomical preparations, followed by Purnobasuki et al. (2017). Compared to floral/reproductive anatomy, vegetative anatomy is more frequently used as a taxonomic characteristic (Hasanuddin and Fitriana 2014). Plant tissue is implanted into paraffin blocks as part of this process to create incredibly thin preparations.

Plant tissue was cut with a thickness of 0.5-1 cm as the first step in the anatomical preparation process. Plant tissue fragments were sucked while fixed in FAA solution (Formalin, Glacial Acetic Acid, and 70% ethanol). Then, a dehydration process employing varying concentrations of alcohol (50, 70, 95, and 100%) and a dealcoholization procedure using a clearing agent like xylol were carried out. Then, a planting media made of paraffin that had been frozen in an incubator was used in place of the purifying medium (infiltration). Plant tissue was inserted into paraffin blocks, which were sliced into thin bands using a microtome after the paraffin block solidified and formed into a trapezium. On a glass object that has been covered in albumin, the paraffin band will be attached. The thin paraffin band is colored with safranin and fast green in the final phase, after which the object-glass is covered with a cover glass. Anatomical specimens will be examined with a light microscope to provide a stunning 200-400x magnification of the tissues (Santos et al. 2016; Susetyarini et al. 2019).

DNA barcoding

DNA extraction

The material used for DNA extraction is young leaves of *C. caudatus* located on the shoots. The leaves are cut into small pieces and weigh 0.1 g. The Tiangen Plant Genomic DNA Kit and associated procedure were used to isolate DNA. Thermo Scientific Multiskan Go was used to check the extracted DNA's concentration and purity.

Amplification and sequencing

Amplification of *rbcL* and *matK* genes assisted by PCR (Polymerase Chain Reaction) using two different specific primers. They are primers *rbcL* (Forward: 5'AAGTTCCTCCACCGAACTGTAG 3' and Reverse: 5'TACTGCGGGTACATGCGAAG 3') and *matK* (Forward: 5' TGGTTCAGGCTCTTCGCTATTG 3' and Reverse: 5'CTGATAAATCGGCCCAAATCGC 3'). Both primers were designed specifically for the Asteraceae family using Primer3 (Rozen and Skaletsky 2000). PCR mixtures were performed in a volume of 35 µL containing the mixture consisting of 7.5 µL GoTaq® Green Master Mix, 1.5 µL of each forward and reverse primer with a concentration of 350-500 nM, 5 µL of 50 ng^{-1} DNA template, and added with nuclease-free water until the solution volume reaches 35 µL.

DNA amplification using a PCR thermocycler that is set using certain parameters. The PCR program for amplification of the *rbcL* and *matK* genes was set into 5 stages, including pre-denaturation at 94°C for 5 minutes, 35 cycles for denaturation at 94°C for 30 seconds, annealing at 56°C for 45 seconds and extension at 72°C for 45 seconds, final extension at 72°C for 5 minutes, and soaking at 4°C. The PCR products of the *rbcL* and *matK* genes were checked to see whether they are amplified as expected or not. Checking is done by visualizing the PCR product on a UV transilluminator using 1% agarose and 0.5 X Tris Borate EDTA (TBE). Subsequently, sequencing the PCR products were performed at the 1st Base Sequencing Service (Axil Scientific Pte. Ltd. Singapore).

Data analysis

Morphological and anatomical investigations were analyzed descriptively. The forward and reverse sequences for the successfully sequenced *rbcL* and *matK* genes were aligned using the Bioedit 7.4 program to produce high-quality DNA consensus data. The proportion of nitrogen

bases in each gene is also calculated using Geneious 2021.3.4 software.

The consensus sample data will undergo multiple sequence alignment using the BLAST online tool (https://blast.ncbi.nlm.nih.gov), which will be used to compare the consensus sample data to the Asteraceae sequence found in the GenBank database. Mega X software will be used to assemble the phylogenetic tree from sample plant sequences and Asteraceae plant sequences received from the BLAST tool. The method used to reconstruct the phylogenetic tree is the Neighbor-Joining Method algorithm approach. The NJ (neighbor joining) algorithm is a widely used method for constructing phylogenetic trees based on the distance between species (Hong et al. 2021). The data used to construct the phylogenetic tree were *rbcL* and *matK* gene sequences from the sample plant *C. caudatus* and 12 sequences of the Asteraceae family which were closely related to the sample plants (Table 1).

RESULTS AND DISCUSSION

Morphological characters

Based on morphological investigations, *Cosmos caudatus* is an annual plant (Sekar et al. 2014) with a shrub habit (Huynh et al. 2021) and it grows in clusters (Uzbek and Shahidan 2019) (Figure 1A). The species has whitish brown taproots (Nurmalasari et al. 2020) (Figure 1B). *C. caudatus* has an erect stem with a rectangular shape and oblong (Utami 2008). The stems are mostly green, but some areas sometime have a purple or reddish color. The purple color is due to the presence of anthocyanins and more branches on the top of the stem than on the bottom (Bunawan et al. 2014; Saleh et al. 2020; Huynh et al. 2021) (Figures 1C, 1D and 1E). Du et al. (2015) stated anthocyanin content is one of the substances that affect stem color. Anthocyanins are beneficial for human health, as bioactive compounds that can be useful for preventing various chronic diseases (Priska et al. 2018).

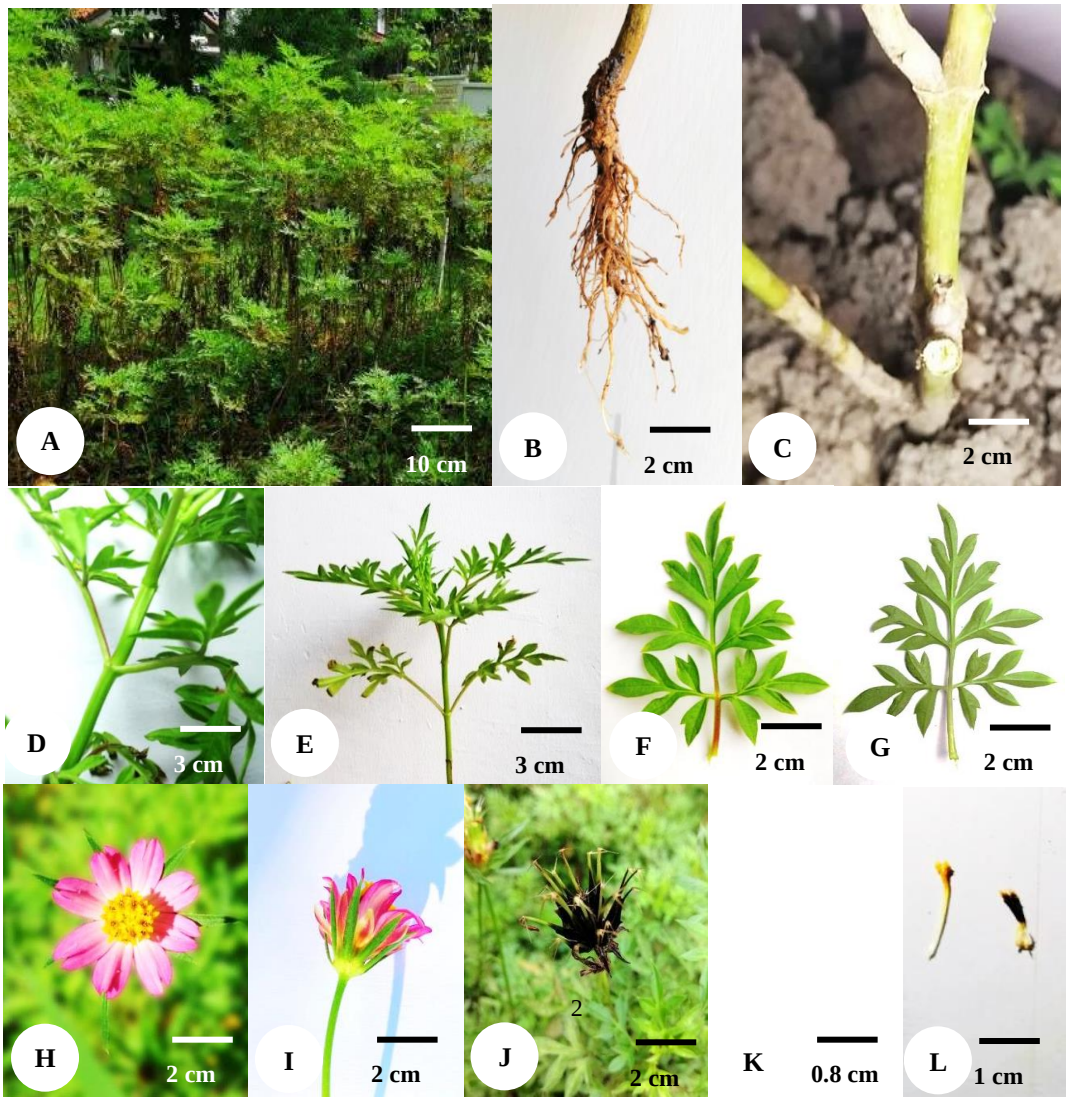

Figure 1. Morphology of *Cosmos caudatus*. A. Habit, B. Taproot, C. Lower stem, D. Middle stem, E. Upper stem, F. Upper leaf surface, G. Lower leaf surface, H. Inflorescence when viewed from above, I. Compound flower when viewed from the side, J. Frui, K. Seeds, L. Pistil and stamen from disc floret

Table 1. DNA sequence data downloaded from GenBank used in the study

Plant species (*rbcL*)	**Accession (*rbcL*)**	**Plant species (*matK*)**	**Accession number (*matK*)**
Cosmos bipinnatus Cav.	KM218349.1	*Cosmos sulphureus* Cav.	EU049362.1
Cosmos bipinnatus Cav.	AB530960.1	*Cosmos caudatus* Kunth	JQ586821.1
Bidens pilosa L.	MH767488.1	*Coreopsis verticillata* L.	EU049356.1
Bidens frondosa L.	MF135475.1	*Coreopsis latifolia* Michx.	AY551482.1
Bidens frondosa L.	MF135468.1	*Coreopsis pulchra* F.E.Boynton	AY551481.1
Bidens alba (L.) DC.	MF135349.1	*Coreopsis delphiniifolia* Lam.	AY551478.1
Bidens pilosa L.	MF135334.1	*Bidens pilosa* L.	MF159461.1
Bidens tripartita L.	NC_058915.1	*Bidens pilosa* L.	MF159439.1
Coreopsis major Walter	KJ773400.1	*Bidens alba* (L.) DC.	MF159414.1
Coreopsis sp.	AB586217.1	*Bidens pilosa* L.	KU958568.1
Bidens cosmoides Sherff	NC_047278.1	*Bidens alba* var. *radiata* (Sch.Bip.) R.E.Ballard	HM989732.1
Bidens macrocarpa Sherff	NC_047274.1	*Bidens hintonii* (Sherff) Melchert	EU049354.1

The leaves are arranged opposite, pinnate, and are divided into 5 leaflets. These characteristics are similar to Chan et al. (2017) and Murugesu et al. (2020) (Figures 1D and 1E). The leaf segments are oblong to lance shaped (Bunawan et al. 2014) with flat leaf edges and pointed leaf tips (Widyawati and Zulchi 2019). The leaf surface has a different color, the abaxial side has a darker color while the adaxial side has lighter color. These characteristics are in accordance with Widyawati and Zulchi (2019) (Figures 1F and 1G). According to Tahir et al. (2017), variations in size, shape, and arrangement of leaves can be an important and interesting source of information in the taxonomy field.

Flowers of Asteraceae have conspicuous features that are important at the family level, such as branches of style, pappus, shape of corolla, and anthers (Batista and De Souza 2017). *C. caudatus* bears compound blooms grouped in a cup, similar to most other Asteraceae plants (Syah et al. 2014). The flower stalk is ±25 cm in length (Fitmawati and Erwina 2017). The compound inflorescence of this plant is surrounded by a bunch of bandage leaves arranged in a tiny hump (involucrum). The involucrum has a bell-like shape (Hidayat et al. 2008) with green in color and a pointed tip. The plants have blooms that develop in the axils of the top leaves or on the tops of the stems. There are typically two different types of flowers in one hump, namely disk flowers (tubular flowers) in the center and ray flowers (flowers with ribbon-like shapes) on edge (Lawrence 1968) (Figures 1H and 1I).

Ray flowers are generally eight pieces, purple or reddish color, but it is sometimes greenish-yellow color with a size of about 1-1.5 cm in length, while the disc flowers have 1 cm in length (Bunawan et al. 2014; Murugesu et al. 2020). The purple fragrance of ray flowers comes from the content of anthocyanin compounds (Gunasekaran et al. 2021) (Figures 1H and 1I). Of the 2 types of flowers, only disc flowers are functional, because they have pistils and stamens. The pistil is covered by fine hairs (Fitmawati and Erwina 2017) and has two branches (Utami 2008). The pistil is yellowish green, while the stamens are tubular with brown anthers (Syah et al. 2014) (Figure 1L). Ray flower is unisexual (Arnold et al. 2014; Rahman 2013). According to Gillies et al. (2002) and Schilling (2006), ray flowers have the function of increasing the attention of pollinators.

The blossoms will eventually turn into fruit after the pollination. The fruit has a hard texture (Utami 2008) with black color and 1-3 cm in length. Each fruit contains a single seed, and the upward-facing tip of the fruit has a structure resembling an arrowhead that is made up of 2-3 pieces. This finding is similar to Bunawan et al. (2014) (Figure 1J). *C. caudatus* seeds are small, 1 cm in length, hard texture (Utami 2008), and needle-shaped brown with a hairy tip (Van den Bergh 1994) (Figure 1K).

Anatomical characters

Cosmos caudatus exhibited all of the confirmed adult ground tissue. The epidermis, cortex, and stele were observed in *C. caudatus* root (Figure 2A). Root epidermal cells are oval. Compared to the underlying tissue, the arrangement of epidermal cells is denser and there is no intercellular space. The inside of the root can be protected from various soil disturbances due to this structure. An intact epidermis is crucial for certain key processes in plant development, shoot growth, and defense (Javelle et al. 2011).

The parenchyma cells that make up *C. caudatus* cortex are smaller than the epidermis, have gaps between them, and are rectangular. Root cortical tissue plays a fundamental role in permitting plants to cope with various environments (Di Ruocco et al. 2018). According to Shaheen et al. (2018), the stele which contains the vascular bundles and pith is the deepest part found in the root. *C. caudatus* has a stele of the tetrarchradial kind, as reported by da Silva Santos et al. (2014) in *Cosmos sulphureus.* The arrangement of the xylem and phloem on the tetrarchradial stele alternates their positions. Xylem tissue occupies most of the space in the root. This is similar to the root tissue in *Ageratum conyzoides* (Santos et al. 2016).

The stem of *C. caudatus* consists of 4 tissues, namely epidermis, cortex, transport tissue (Figure 2B) and pith (Figure 2C). The epidermis is rectangular and has one layer of densely packed cells. In addition to protecting plants from infections and dehydration, the shoot epidermis is crucial for appropriate organogenesis and growth regulation (Takada and Iida 2014). The cortical tissue

which lies beneath the epidermis comprises parenchyma cells with rectangular form. The transported tissue of *C. caudatus* is of the open collateral type (Jannah et al. 2021), consisting of several continuous bundles and distributed in a single ring (Santos et al. 2016) with the interfascicular cambium existing between the xylem and phloem (Ilham et al. 2022). The deepest portion of the stem is made up of pith tissue, just like roots. The pith is made up of undifferentiated parenchyma cells and serves as a nutrient storage system in eudicot (Kirkendall et al. 2015)

Leaves consist of 3 tissues, namely epidermal tissue, mesophyll, and transport tissue (Figures 2D and 2E). The leaf epidermis is composed of 2 layers, each on the upper and lower sides. The epidermis consists of a single layer of cells arranged tightly (uniseriate) with an oval to rectangular shape. *Cosmos parviflorus* also has a uniseriate epidermis (Rivera et al. 2019). Epidermal cells in leaves are not always arranged tightly. Stomata of *C. caudatus* have a position parallel to the epidermis, as in *C. bipinnatus* (Rivera et al. 2019). The mesophyll tissue of *C. caudatus* is heterogeneous because it has 2 different tissues, namely palisade tissue and spongy tissue. The characteristics of the mesophyll tissue of this plant are similar to that of *C. parviflorus*, but in contrast to the homogeneous mesophyll tissue of *C. bipinnatus* (Rivera et al. 2019). The adaxial side of the mesophyll tissue contains a single layer of elongated and dense cells that make up the palisade tissue. In contrast, the sponge tissue comprises 3-4 layers of loosely distributed cells positioned on the abaxial side. The vascular bundles in the leaves are arranged in a collateral type, the same for C. *parviflorus* (Rivera et al. 2019).

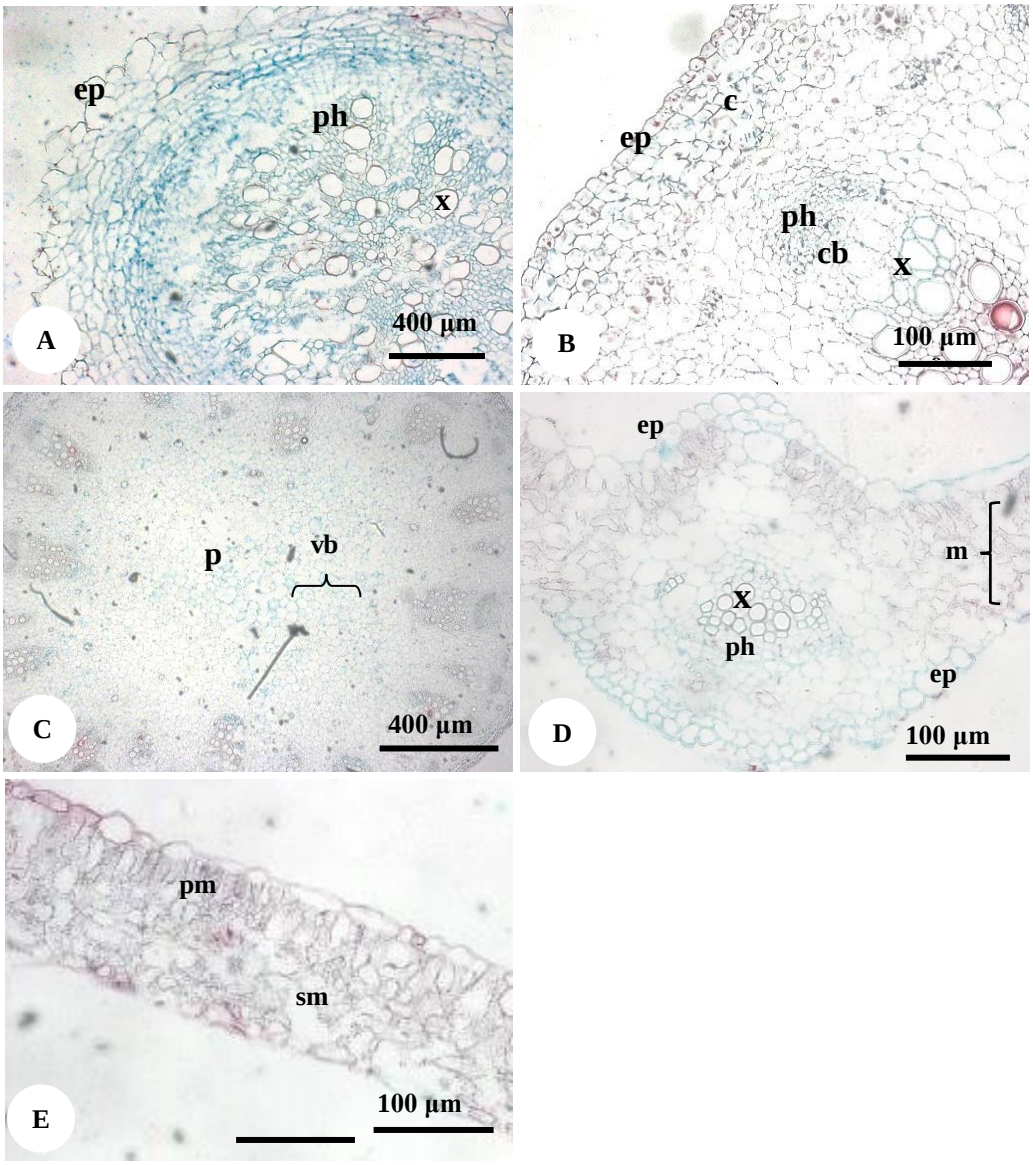

Figure 2. Anatomy of *Cosmos caudatus*. A. Root 200X, B. Stem 400X, C. Stem 200X, D-E. Leaf 400X. ep: epidermis, c: cortex, p: pith, x: xylem, ph: phloem, m: mesophyll, pm: palisade mesophyll, sm: spongy mesophyll, cb: cambium, vb: vascular bundles

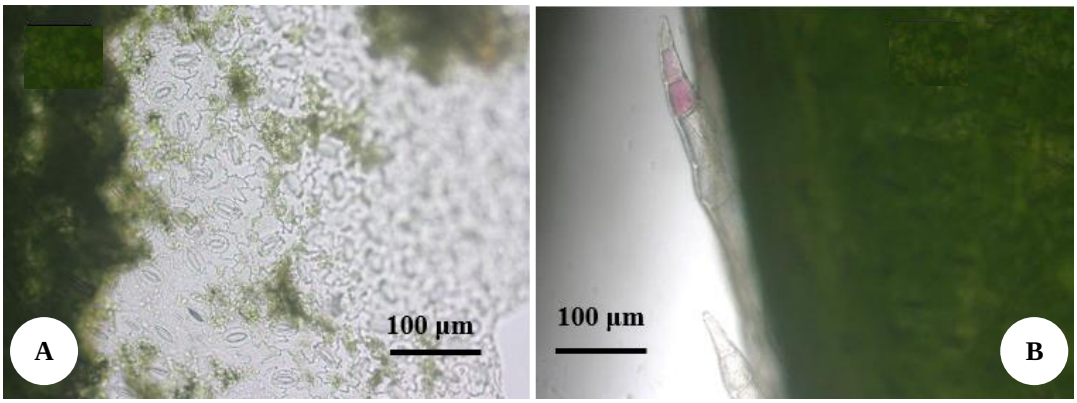

Figure 3. Leaves anatomy of *Cosmos caudatus*. A. Stomata 400X, B. Trichome 400X

Leaves have various important characteristics that can be used as markers for identifying plant species (Stace 1984), especially the epidermal structures that undergo differentiation into accessory tissues. The epidermal cell walls, stomatal types, and trichomes of leaves are key factors at both the generic and particular levels in many groups of plants (Rahman et al. 2013; Srilakshmi et al. 2014). According to Metcalfe and Chalk (1979), type of stomata, trichomes, papillae, hydathodes, and bundle vessels are the anatomical traits that can be seen in the Asteraceae family. Tahir et al. (2017) reported that stomata characteristics are significant taxonomic tools for identifying species.

Cosmos caudatus under study had anomocytic and anisocytic stomata (Figure 3A), which is similar to previous study reported by Rahman et al. (2013). This result is also supported by Srilakshmi and Naidu (2014) from three Asteraceae species, the same leaf surface can have two different stomata combinations. Sari and Harlita (2018) claimed that *C. caudatus* possesses anisocytic stomata, however, Hasanuddin and Fitriana (2014) and Jannah et al. (2021) reported that *C. caudatus* has an anomocytic stomata type. Compared with other species in the same genus, *C. sulphureus* only has one type of stomata, anisocytic (Tahir et al. 2017). Much evidence from the fossil record of Angiosperms and many other seed plants suggest that anomocytic stomata are the ancestor of all known stomata types. Actinocytic stomata were first known to evolve from the anomocytic type (Carpenter 2005).

Other leaf epidermal-derived cells that can be used as additional information for identifying a species is trichome, because it varies in size and show different shapes (Glas et al. 2012). Perveen et al. (2016) reported that the size and shape of trichome could be used for classification in 17 species of Asteraceae family. Adedeji and Jewoola (2008) also presented that trichomes have been successfully used to delimit several genera in the Asteraceae family.

Trichomes in *C. caudatus* are composed of several cells with pointed apical cells, like horns (Figure 3B). This result is consistent with the research of Sari et al. (2021) that of the 8 Asteraceae species studied, all species have glandular trichomes with pointed ends. In certain areas, the trichome cells have a purple color, which appears due to the anthocyanin content, indicating that they are of the glandular kind. According to Gunasekaran et al. (2021), flower trichomes also have a purplish-red pigment.

Glandular trichomes are an important source of essential oils, such as natural fragrances or products that can be used by the pharmaceutical industry. However, many of these substances have evolved to provide the plant with protection against herbivores and pathogens (Glas et al. 2012). Glandular trichomes also have other functions, including controlling the release of water through the secretion of essential oils. The secretions produce a thick layer that can prevent water vapor loss (Carmona and Ancibor 1995; Molares et al. 2009). Studies of leaf epidermis has gained much importance during this century, because these studies are widely recognized in taxonomy and identifying plant materials in paleobotany, pharmacognosy, and forensic science (Srilakshmi and Naidu 2014).

DNA barcoding

PCR amplification and sequencing

The *rbcL* and *matK* genes were successfully amplified and each individual has presented in various sizes. The *rbcL* gene has a size of approximately 500 bp (Figure 4A) and *matK* has a size of approximately 750 bp (Figure 4B). The visualization results are not much different from the research conducted by Ilham et al. (2022), in which *rbcL* gene in *Achillea millefolium* has a size of approximately 500 bp and *matK* has a size of 750 bp. Those studies used the same primer, which was also used by Wahyuni et al. (2019).

The *rbcL* and *matK* genes have a fairly good thickness of the amplified DNA band (Figures 4A and 4B). According to Michel et al. (2016), dense and agglomerated DNA bands showed a high quantity. The thickness of the visualized DNA bands depends on several factors, such as primers, annealing temperature, and concentration of DNA polymerase. Primers are designed to increase two significant base sequence specificity and reasonable GC content indicators.

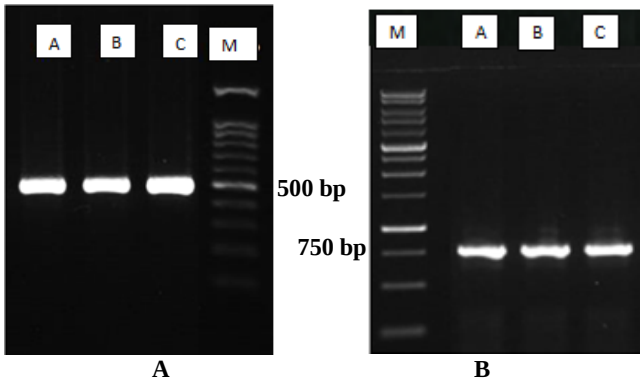

Figure 4. Amplification results. A. *rbcL* gene, B. *matK* gene. 1: sample 1, 2: sample 2, 3: sample 3, M: marker

The high specificity can prevent mispriming in regions other than the target region, and the GC content of a primer is a major factor in determining the annealing temperature (Tm) (Kayama et al. 2021). In addition, the annealing temperature is a crucial factor in PCR reaction affecting product (gene fragments) specificity (Kurniawati and Hartati 2018). These serve as an extension point for the DNA polymerase to build on. DNA polymerase is also an important enzyme that functions to form new DNA strands in the PCR process (Garibyan and Avashia 2013).

It was discovered that there were no gaps in either the *rbcL* gene (Figure 5A) or the *matK* gene (Figure 5B) after processing the sample plant sequence data using Bioedit 7.4 and Mega X software. In general, gaps in the DNA sequence are caused by insertions and deletions (Fan et al. 2007). In the early stages of eukaryotic evolution, insertion and deletion are probably the most significant and fast types of sequence change (Sanyal et al. 2015). Point mutations encompass both varieties of mutations. According to Flint-Garcia (2013), a mutation is a set of irreversible changes that occur in an organism's gene or nucleotide sequence. The gene alteration might impact one nucleotide (point mutation) or numerous nearby nucleotides (segmental mutation). The base population is created by mutation, followed by an increase in the population's genetic diversity. In other words, genetic variety is a foundational population for evolution through natural selection (Maruzy et al. 2020). Therefore, gaps in DNA barcoding are not a sign of failure, rather, they can be used to forecast whether DNA barcoding will be successful for the taxon under study (Keskin and Atar 2013).

Comparisons of gene sequences within species were also carried out on species of different genera with genetic distances that were considered quite far from the sample plants. The purpose of this comparison is to determine whether there are differences in the composition of nitrogen bases between 2 distantly related taxon. For the *rbcL* gene, comparisons were made using *Bidens cosmoides* accession NC 047278.1, while for the *matK* gene using *B. pilosa* accession MF159439.1.

It turns out that there are several differences in nucleotide variations, the most differences being in the *matK* gene. The *rbcL* gene comparison reveals seven different nucleotide changes, specifically at nucleotide numbers 250, 313, 344, 400, 412, 631, and 685 (Figure 5A). While in comparison using the *matK* gene, nucleotide variations are found in nitrogen bases number 115, 207, 256, 257, 282, 331, 332, 364, 374, 446, and 574 (Figure 5B).

DNA sequence

The *rbcL* gene in samples 1, 2, and 3, each had adenine percentage of 29.1-29.4%, guanine 19.3-19.5%, thymine 26.8-26.9%, and cytosine 24.2-24.7%. While the *matK* gene has a percentage of 36.5-36.6% adenine, 17.2% guanine, 29.2-29.3% thymine, and 17% cytosine (Table 2). Adenine and thymine appear to have total dominance in the *rbcL* and *matK* genes based on a study of the number of nitrogen bases. This result is in line with Smith et al. (2011) that adenine and thymine comprise most of the mitochondrial and plastid genome sequences. Wahyuni et al. (2019) also reported that the proportion of GC has a smaller concentration than AT (guanine of 42.7% and cytosine of 35.4%).

Based on the *rbcL* gene, sample 1 had 472 bp, sample 2 had a nitrogen base of 477 bp and sample 3 had the largest amount, 483 bp. Whereas in the *matK* gene, samples 1 and 3 had 702 bp, and sample 2 had 699 bp

The sequences of *C. caudatus* used in the study and *C. bipinnatus* accession KM218349.1 and accession AB530960.1 show striking similarities in the BLAST results based on the *rbcL* gene (Table 3). The GenBank database's information on the *C. caudatus rbcL* gene is currently lacking as of 13/06/2022. The sample plants shared similarities with *C. sulphureus* accession EU049362.1 and *C. caudatus* accession JQ586821.1, according to the BLAST results based on the *matK* gene in Table 4. The degree of similarity is calculated based on the % identity, query cover, and e-values.

The sample sequences and several sequences from GenBank described above have a 98-100% identity rate. When a significant percentage of identity between a gene sequence from an unknown species and a gene sequence from a species that has been recognized is found, the two gene sequences are classed as belonging to the same species (Lis et al. 2016). The e-value between the sample plants and a few of the sequence mentioned above is zero. According to Tindi et al. (2017), a significant sequence alignment is indicated by an e-value of 0. E-Value 0 denotes that the gene sequence of the sample organism and the gene sequence found in the GenBank database are the same (Sogandi 2018). Query cover BLAST results have a value of 96-100%. According to Fathiya et al. (2018), query cover refers to the percentage of nucleotide length from the sample organism that agrees with the sequence of organisms in the GenBank database (Nugraha et al. 2014). Homology in genetics refers to genes that share the same nitrogen base sequence. The sample sequences are considered to be comparable to the sequence found in GenBank if the max score and total score are the same, query cover is close to 100%, e-value is close to 0, and percentage identity is close to 100% (Tindi et al. 2017).

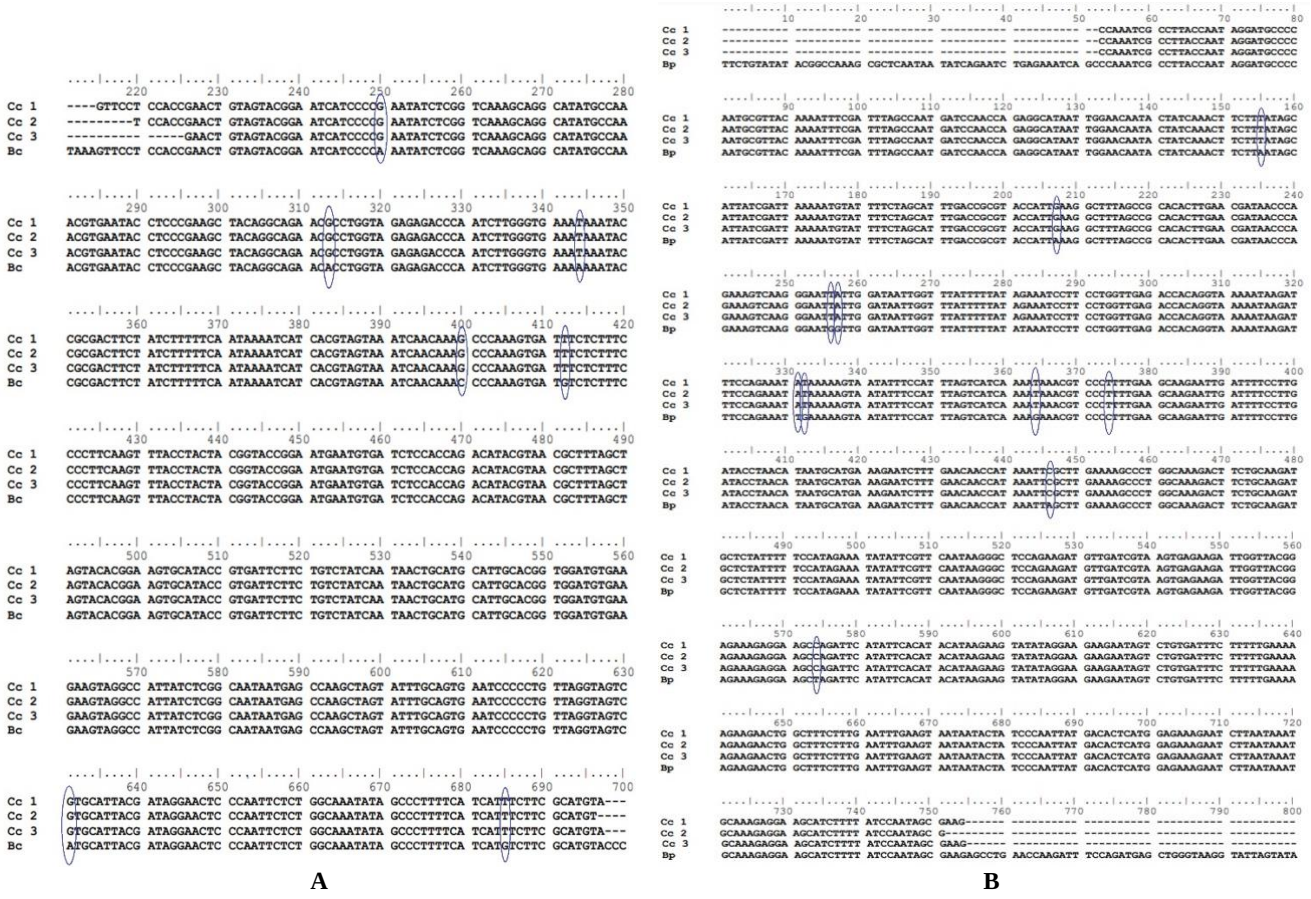

Figure 5. Comparison of the sequence of *Cosmos caudatus* being studied with several plant sequences from the genus *Biden*s. A. Compared with *B. cosmoides* accession NC_047278.1, *rbcL* gene, B. Compared with *B. pilosa* accession MF159439.1, *matK* gene. The blue circle indicates the presence of nucleotide differences (variations). (Bp: *B. cosmoides*, Bp: *B. pilosa*)

The *rbcL* and *matK* genes are commonly utilized as DNA barcode standards. These two genes have an advantage over nuclear DNA, because they fall under the category of chloroplast DNA. For example, chloroplast DNA has a low evolutionary rate and is frequently used to identify relatives among Angiosperm species, whereas nuclear DNA has more genetic variation because of its high recombinant rate (Anzani et al. 2021). According to Kang et al. (2017), the four genes utilized as DNA barcode markers for species in tropical cloud forests (*rbcL*, *matK*, *trnH-psbA*, and ITS), *rbcL*, and *matK* showed relatively high amplification levels, sequencing success rates, and identification success rates. The *rbcL* exhibits a rather high amount of amplification when compared to *matK* (Hollingsworth et al. 2016). Compared to the *matK* gene, the *rbcL* gene shows strong intraspecific and moderate interspecific divergence (Ho et al. 2021).

The *matK* gene has a higher species discrimination ability than *rbcL*, since variations in the *rbcL* sequence are most commonly found at levels above species (Newmaster et al. 2006; Kress and Erickson 2007; Sass et al. 2007; Fazekas et al. 2008). Therefore, the *rbcL* gene is being employed extensively for phylogenetic analysis at the level of families and subclasses of Angiosperms and among various groups of seed plants (Chase et al. 2007). Saarela et al. (2013) reported that for 490 vascular plant species, *matK* was more divergent than *rbcL* at both the intraspecies and interspecies levels.

Phylogenetic analysis

The phylogenetic trees constructed by *rbcL* and *matK* genes are presented in Figure 6. The three samples of *C. caudatus* in Figures 6A and 6B are located in the same group with identical branch lengths. Furthermore, identical branch sizes between taxa groups showed no significant changes in nucleotide sequence (Ilham et al. 2022), so it can be considered to have a very close genetic relationship. This result is in accordance with Anzani et al. (2021) that groups of taxa located in the same branch have a very close level of relationship.

Table 2. Comparison of the number of nitrogenous bases in *Cosmos caudatus*

Samples	Percentage of nitrogen bases	Number of nitrogen bases
C. caudatus rbcL 1	A: 29.4%, G: 19.5%, T: 26.9%, C: 24.2%	472
C. caudatus rbcL 2	A: 29.1%, G: 19.3%, T: 26.8%, C: 24.7%	477
C. caudatus rbcL 3	A: 29.1%, G: 19.3%, T: 26.8%, C: 24.7%.	483
C. caudatus matK 1	A: 36.6%, G: 17.2%, T: 29.2%, C: 17%.	702
C. caudatus matK 2	A: 36.5%, G: 17.2%, T: 29.3%, C: 17%.	699
C. caudatus matK 3	A: 36.6%, G: 17.2%, T: 29.2%, C: 17%.	702

Table 3. Summary of alignment results of *rbcL* using BLAST

Scientific name	Max score	Total score	Query cover	E value	Per. ident	Accession
Cosmos bipinnatus	872	872	100%	0	100.00%	KM218349.1
Cosmos bipinnatus	872	872	100%	0	100.00%	AB530960.1
Bidens pilosa	839	839	100%	0	98.73%	MH767488.1
Bidens frondosa	839	839	100%	0	98.73%	MF135475.1
Bidens frondosa	839	839	100%	0	98.73%	MF135468.1
Bidens alba	839	839	100%	0	98.73%	MF135349.1
Bidens pilosa	839	839	100%	0	98.73%	MF135334.1
Bidens tripartita	839	839	100%	0	98.73%	NC_058915.1
Coreopsis major	839	839	100%	0	98.73%	KJ773400.1
Coreopsis sp.	839	839	100%	0	98.73%	AB586217.1
Bidens cosmoides	833	833	100%	0	98.52%	NC_047278.1
Bidens macrocarpa	833	833	100%	0	98.52%	NC_047274.1

Table 4. Summary of alignment results of *matK* using BLAST

Scientific name	Max score	Total score	Query cover	E value	Per. ident	Accession
Cosmos sulphureus	1286	1286	100%	0	99.86%	EU049362.1
Cosmos caudatus	1253	1253	96%	0	100.00%	JQ586821.1
Coreopsis verticillata	1236	1236	100%	0	98.57%	EU049356.1
Coreopsis latifolia	1236	1236	100%	0	98.57%	AY551482.1
Coreopsis pulchra	1236	1236	100%	0	98.57%	AY551481.1
Coreopsis delphiniifolia	1236	1236	100%	0	98.57%	AY551478.1
Bidens pilosa	1230	1230	100%	0	98.43%	MF159461.1
Bidens pilosa	1230	1230	100%	0	98.43%	MF159439.1
Bidens alba	1230	1230	100%	0	98.43%	MF159414.1
Bidens pilosa	1230	1230	100%	0	98.43%	KU958568.1
Bidens alba var. *radiata*	1230	1230	100%	0	98.43%	HM989732.1
Bidens hintonii	1230	1230	100%	0	98.43%	EU049354.1

The *rbcL* and *matK* genes also seem to be able to group each specimen into the right taxonomic group at the genus level. Several sequences of different *Cosmos* species are in the same branch group and are separated from other species, which incidentally are different genera. Exception in the *rbcL* phylogenetic tree, *Coreopsis* sp. accession AB586217.1 and *Coreopsis major* accession KJ773400.1 are not located in the same group and are separate from each other. Based on the *rbcL* gene, *C. caudatus* used in the study was in the same branch group as *C. bipinnatus* accessions KM218349.1 and AB530960.1 (group A) (Figure 6A). Meanwhile, in the *matK* gene, the plants studied were in the same group (group B) *with C. sulphureus* accession EU049362.1 and *C. caudatus* accession JQ586821.1 (Figure 6B). Both groups A and B can be separated from the genera *Bidens* and *Coreopsis.* It seems that using a combination of the two genes is better to determine the position of a species at a certain taxon level. This result is supported by Ho et al. (2021) that the combination of the *rbcL* and *matK* loci can significantly increase the separability. The *rbcL* and *matK* genes have better resolution and homology than other genes and ITS (Rohimah et al. 2018; Perwitasari et al. 2019). As an instance, species of the genus *Zanthoxylum* can be grouped and distinguished from other genera using the *matK* gene marker (Manurung et al. 2018).

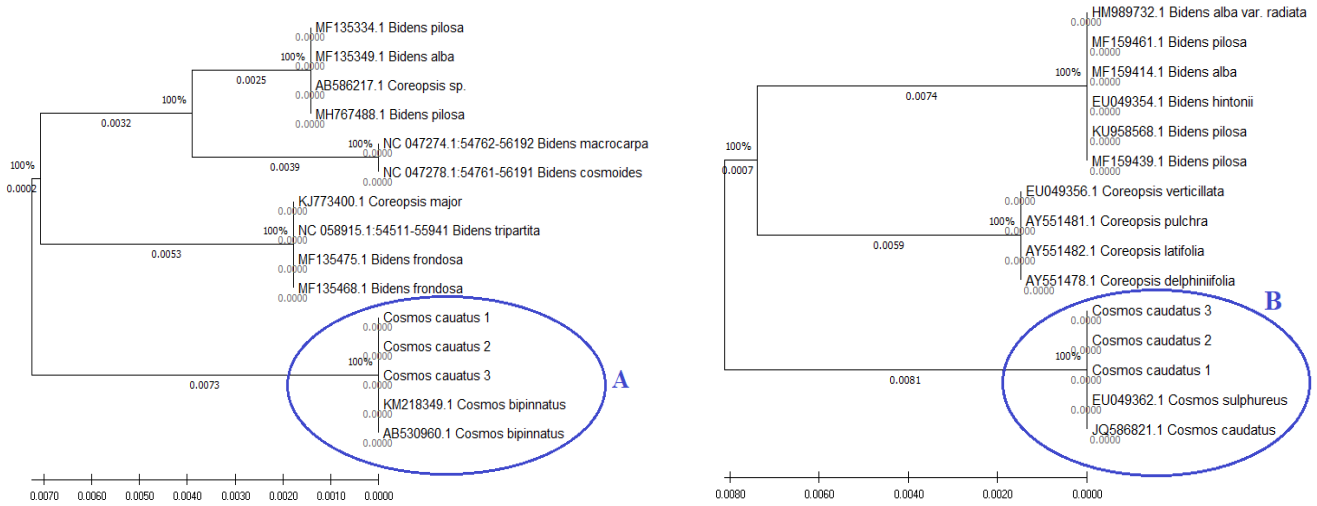

A **B**

Figure 6. The phylogenetic tree generated. A. *rbcL* gene, B. *matK* gene

In conclusion, the roots of C. *caudatus* are tapped type with erect stems with a slightly purplish green color. The leaves are classified as pinnate compounds with two colors on the adaxial and abaxial sides. Compound flowers of *C. caudatus* are cup-type with two kinds of flowers that differ in form and function, namely disc flowers and ray flowers. Based on anatomical observation, the roots and stems of *C. caudatus* are the same as in shrub dicotyledonous plants in general, with a characteristic root having a tetrarchradial type stele. Leaf anatomy showed the presence of heterogeneous mesophyll, glandular trichomes and stomata of multiple types, namely anomocytic and anisostitic. *C. Caudatus* showed a very high genetic affinity with many plants of the *Cosmos* genus downloaded from the GenBank database. The phylogenetic trees place the studied plants with plants of the *Cosmos* genus into the same group.

ACKNOWLEDGEMENTS

We thank LIPJPHKI (Lembaga Inovasi, Pengembangan Jurnal, Penerbitan dan Hak Kekayaan Intelektual) Universitas Airlangga for their assistance during the preparation of this manuscript, LPPM Universitas Airlangga for all funding administration, collaboration scheme and research legality assistance. This study was financially supported by Hibah Riset Kolaborasi Indonesia 2021, Grant No: 5./RKI/Thp-I/2021.

REFERENCES

Adedeji O, Jewoola OA. 2008. Importance of leaf epidermal characters in the Asteraceae family. Notulae Botanicae Horti Agrobotanici Cluj-Napoca 36: 7-16.

Ajaykumar TV, Anandarajagopal K, Sunilson JAJ, Arshad A, Jainaf RAM, Venkateshan N. 2012. Anti-inflammatory activity of *Cosmos caudatus*. Intl J Univers Pharm Bio Sci 1 (2): 40-48.

Anzani AN, Martiansyah I, Yuliani N. 2021. In silico study of DNA barcoding on soka flower (*Ixora*). Pros Biol Achiev the Sustain Dev Goals with Biodivers in Confront Climat Chang 7 (1): 168-177. DOI: 10.24252/psb.v7i1.23693. [Indonesian]

Arnold R, Tiwari S, Saxena A, Mishra RM, Anand P, Pandey R. 2014. Ecological studies of natural populations of *Cosmos caudatus*, H. with special reference to pollination, seed behavior and biomass distribution. J Chem Biol Phys Sci Sec B Biol Sci 4 (1): 324-328.

Batista MF, De Souza LA. 2017. Flower structure in ten Asteraceae species: Considerations about the importance of morpho-anatomical features at species and tribal level. Braz J Bot 40: 265-279. DOI: 10.1007/s40415-016-0312-9.

Bodeker G. 2009. Health and Beauty from the Rainforest: Malaysian Traditions of Ramuan. Didier Millet, Kuala Lumpur.

Bunawan H, Baharum S, Bunawan SN, Amin NM, Noor NM. 2014. *Cosmos caudatus* Kunth: A traditional medicinal. Glob J Pharmacol 8 (3): 420-426. DOI: 10.5829/idosi.gjp.

Carmona CS, Ancibor E. 1995. Anatomía ecológica de las especies de Acantholippia (Verbenaceae). Bol Soc Argent Bot 31 (1-2): 3-12.

Carpenter KJ. 2005. Stomatal architecture and evolution in basal Angiosperms. Am J Bot 92 (10): 1595-1615. DOI: 10.3732/ajb.92.10.1595.

Chan E, Wong S, Chan H. 2017. Ulam herbs of *Oenanthe javanica* and *Cosmos caudatus*: An overview on their medicinal properties. J Nat Remedies 16 (4): 137-147. DOI: 10.18311/jnr/2016/8370

Chase MW, Cowan R, Hollingsworth PM, Berg CV, Madriñán S, Petersen G, Seberg O, Jørgsensen T, Cameron KM, Carine M, Pedersen N, Hedderson TA, Conrad F, Salazar GA, Richardson JE, Hollingsworth ML, Barraclough TG, Kelly LJ, Wilkinson M. 2007. A proposal for a standardised protocol to barcode all land plants. Taxon 56 (2): 295-299. DOI: 10.1002/tax.562004.

Chen S, Pang X, Song J, Shi L, Yao H, Han L, Leon C. 2014. A renaissance in herbal medicine identification: from morphology to DNA. Biotechnol Adv 32 (7): 1237-1244. DOI: 10.1002/tax.562004.

Cheng S-H, Barakatun-Nisak MY, Anthony J, Ismail A. 2015. Potential medicinal benefits of *Cosmos caudatus* (Ulam Raja): A scoping review. J Res Med Sci 20 (10): 1000-1006. DOI: 10.18311/jnr/2016/8370.

Christenhusz MJM, Byng JW. 2016. The number of known plants species in the world and its annual increase. Phytotaxa 261 (3): 201-217. DOI: 10.11646/phytotaxa.261.3.1.

Da Silva Santos L, Dariva HS, Muller RH, Odair JGDA, de Souza LA. 2014. Seedling structure in Asteraceae weedy species: Considerations on the vasculature system. Braz J Bot 37 (4): 631-635. DOI: 10.1007/s40415-014-0091-0.

De Boer HJ, Ichim MC, Newmaster SG. 2015. DNA barcoding and pharmacovigilance of herbal medicines. Drug Saf 38 (7): 611-620. DOI: 10.1007/s40264-020-01029-9.

Di Ruocco G, Di Mambro R, Dello Ioio R. 2018. Building the differences: A case for the ground tissue patterning in plants. Proc Biol Sci 285 (1890): 20181746. DOI: 10.1098/rspb.2018.1746.

Du H, Wu J, Ji KX, Zeng QY, Bhuiya MW, Su S, Shu QY, Ren HX, Liu ZA, Wang LS. 2015. Methylation mediated by an anthocyanin, o-methyltransferase, is involved in purple flower coloration in *Paeonia*. J Exp Bot 66 (21): 6563-6577. DOI: 10.1093/jxb/erv365.

Fan Y, Wang W, Ma G, Liang L, Shi Q, Tao S. 2007. Patterns of insertion and deletion in mammalian genomes. Curr Genom 8 (6): 370-378. DOI: 10.2174/138920207783406479.

Fathiya N, Harnelly E, Thomy Z, Iqbar. 2018. Molecular identification of *Shorea johorensis* in Ketambe Research Station, Gunung Leuser National Park. J Nat 18 (2): 56-64. DOI: 10.24815/jn.v18i2.10123.

Fazekas AJ, Burgess KS, Kesanakurti PR, Graham SW, Newmaster SG, Husband BC, Percy DM, Hajibabaei M, Barrett SCH. 2008. Multiple multilocus DNA barcodes from the plastid genome discriminate plant species equally well. PLoS ONE 3 (7): e2802. DOI: 10.1371/journal.pone.0002802.

Fitmawati, Erwina J. 2017. Medicinal Plants from Bushes Become Medicine. UR Press, Pekanbaru. [Indonesian]

Flint-Garcia SA. 2013. Genetics and consequences of crop domestication. J Agric Food Chemist 61 (35): 8267-8276. DOI: 10.1021/jf305511d.

Garibyan L, Avashia N. 2013. Polymerase chain reaction. J Invest Dermatol 133 (3): 1-4. DOI: 10.1038/jid.2013.1.

Gillies AC, Cubas P, Coen ES, Abbott RJ. 2002. Making raysin the Asteraceae: Genetics and evolution of radiate versus discoid flower heads. In: Cronk QCB, Bateman RM, Hawkins JA. (eds). Developmental Genetics and Plant Evolution. Taylor & Francis, London.

Glas JJ, Schimmel BC, Alba JM, Escobar-Bravo R, Schuurink RC, Kant MR. 2012. Plant glandular trichomes as targets for breeding or engineering of resistance to herbivores. Intl J Mol Sci 13 (12): 17077-17103. DOI: 10.3390/ijms131217077.

Gunasekaran D, Tahir NI, Akbar MA, Basir S, Ismail I, Talip N, Ramzi AB, Baharum SN, Noor NM, Bunawan H. 2021. Discovery of anthocyanin biosynthetic pathway in *Cosmos caudatus* Kunth. using omics analysis. Agronomy 11 (4): 661. DOI: 10.3390/agronomy11040661.

Hasanuddin, Fitriana. 2014. Relationship fenetik 12 species of Asteraceae family members. J Edubio Trop 2 (2): 187-250. [Indonesian]

Hidayat S, Wahyuni S, Andalusia S. 2008. Potentially Ornamental Medicinal Plants Series. Elex Media Komputindo, Jakarta. [Indonesian]

Ho VT, Tran TKP, Vu TTT, Widiarsih S. 2021. Comparison of *matK* and *rbcL* DNA barcodes for genetic classification of jewel orchid accessions in Vietnam. J Genet Eng Biotechnol 19 (1): 93. DOI: 10.1186/s43141-021-00188-1.

Hollingsworth PM, Graham SW, Little DP. 2011. Choosing and using a plant DNA barcode. PLoS ONE 6 (5): e19254. DOI: 10.1371/journal.pone.0019254.

Hollingsworth PM, Li DZ, van der Bank M, Twyford AD. 2016. Telling plant species apart with DNA: from barcodes to genomes. Phil Trans R Soc B 371: 20150338. DOI: 10.1098/rstb.2015.0338.

Hong Y, Mauzo G, Juan W. 2021. ENJ algorithm can construct triple phylogenetic trees. Mol Thera Nucleic Acids 23: 286-293. DOI: 10.1016/j.omtn.2020.11.004.

Huynh XP, Nguyen TV, Nguyen TNQ, Pham VT, Nguyen MT, Tran TKN. 2021. Phytochemical screening, total phenolic, flavonoid contents, and antioxidant activities of four spices commonly used in Vietnamese traditional medicine. Mater Today Proc 56 (3): A1-A5. DOI: 10.1016/j.matpr.2021.12.142.

Ilham M, Mukarromah SR, Rakashiwi GA, Indriati DT, Yoku BF, Purnama PR, Junairiah, Prasongkuk S, Purnobasuki H, Wahyuni DK. 2022. Morpho-anatomical characterizationand DNA barcoding of *Achillea millefolium* L. Biodiversitas 23 (4): 1958-1969. DOI: 10.13057/biodiv/d230430.

Jannah MMN, Wijaya S, Setiawan HK. 2021. Standardization of dried powder of *Cosmos* (*Cosmos caudatus* Kunth) leaves from three different areas. J Pharm Sci Pract 8 (1): 13-15.

Javelle M, Vernoud V, Rogowsky PM, Ingram GC. 2011. Epidermis: The formation and functions of a fundamental plant tissue. New Phytol 189 (1): 17-39. DOI: 10.1111/j.1469-8137.2010.03514.

Kang Y, Deng Z, Zang R, Long W. 2017. DNA barcoding analysis and phylogenetic relationships of tree species in tropical cloud forests. Sci Rep 7 (1): 12564. DOI: 10.1038/s41598-017-13057-0.

Kaur R, Singh D. 2020. Molecular markers a valuable tool for species identification of insects: A review. Ann Entomol 38 (01-02): 1-20.

Kayama K, Kanno M, Chisaki N, Tanaka M, Yao R, Hanazono K, Camer GA, Endoh D. 2021. Prediction of PCR amplification from primer and template sequences using recurrent neural network. Sci Rep 11: 7493. DOI: 10.1038/s41598-021-86357-1.

Keskin E, Atar HH. 2013. DNA barcoding commercially important fish species of Turkey. Mol Ecol Resour 13 (5): 788-797. DOI: 10.1111/1755-0998.12120.

Kirkendall LR, Biedermann PHW, Jordal BH. 2015. Evolution and diversity of bark and Ambrosia beetles. In: Vega FE, Hofstetter RW (eds). Bark Beetles: Biology and Ecology of Native and Invasive Species. Academic Press, Bergen.

Kress WJ, Erickson DL. 2007. A two-locus global DNA barcode for land plants: The coding *rbcL* gene complements the non-coding *trnH-psbA* spacer region. PLoS ONE 2 (6): e508. DOI: 10.1371/journal.pone.0000508.

Kurniawati S, Hartati NS. 2018. Optimization of the annealing temperature with degenerate primer for amplifiation of arginine decarboxylase (ADC) fragment gene from genomic DNA of Maluku Tenggara local cassava. Jurnal Ilmu Dasar 19 (2): 135-142. DOI: 10.19184/jid.v19i2.6261. [Indonesian]

Lawrence GHM. 1968. Taxonomy Vascular Plants. The Macmillan Company, New York.

Lis JA, Lis B, Ziaja DJ. 2016. In BOLD we trust? A commentary on the reliability of specimen identification for DNA barcoding: A case study on burrower bugs (Hemiptera: Heteroptera: Cydnidae). Zootaxa 4114 (1): 83-86. DOI: 10.11646/zootaxa.4114.1.6.

Manurung J, Prakasa H, Tanjung UJ, Harsono T. 2018. Species relationship in genus *Zanthoxylum* using gene sequence of maturase K (*matK*) chloroplast DNA. Jurnal Biosains 4 (2): 69-77. DOI: 10.24114/jbio.v4i2.10166. [Indonesian]

Maruzy A, Jannah DAF, Pitoyo A, Subositi D. 2020. Comparatison study of macroscopic and microscopic characters in three species *Phyllanthus* L. Floribunda 6 (4): 154-166. DOI: 10.32556/floribunda.v6i4.2020.312. [Indonesian]

Mediani A, Abas F, Khatib A, Tan CP. 2013. *Cosmos caudatus* as a potential source of polyphenolic compounds: optimisation of oven drying conditions and characterisation of its functional properties. Molecules 18 (9): 10452-10464. DOI: 10.3390/molecules180910452.

Metcalfe CR, Chalk L. 1979. Anatomy of the Dicotyledons: Systematic Anatomy of Leaf and Stem with a Brief History of Subject. Calaredon Press, Oxford.

Michel CI, Meyer RS, Taveras Y, Molina J. 2016. The nuclear internal transcribed spacer (ITS2) as a practical plant DNA barcode for herbal medicines. J Appl Res Med Aromat Plants 3 (3): 94-100. DOI: 10.1016/j.jarmap.2016.02.002.

Molares S, Gonzalez SB, Ladio A, Agueda Castro M. 2009. Ethnobotany, anatomy and physicochemical characterization of essential oil of *Baccharis obovata* Hook. et Arn. (Asteraceae: Astereae). Acta Bot Bras 23 (2): 578-589. DOI: 10.1590/S0102-33062009000200030.

Moshawih S, Cheema MS, Ahmad Z, Zakaria ZA, Hakim MN. 2017. A Comprehensive review on *Cosmos caudatus* (Ulam Raja): Pharmacology, ethnopharmacology, and phytochemistry. Intl Res J Educ Sci 1 (1): 2550-2158.

Murugesu S, Perumal V, Balan T, Fatinathan S, Selvarajo PD, Rozali MAB, Aziz NIA. 2020. A Review of *Cosmos caudatus* as a promising antidiabetic plant. Malaysian J Med Health Sci 16 (4): 333-343.

Newmaster SG, Fazekas AJ, Ragupathy S. 2006. DNA barcoding in land plants: Evaluation of *rbcL* in a multigene tiered approach. Can J Bot 84 (3): 335-341. DOI: 10.1139/b06-047.

Nugraha F, Roslim DI, Ardilla YP, Herman. 2014. Analysis of partial gene sequence Ferritin2 on rice plants (*Oryza sativa* L.) in Indragiri Hilir, Riau. Biosaintifika 6 (2): 94-103. DOI: 10.15294/biosaintifika.v6i2.3102.

Nurmalasari P, Andyhapsari D, Marizka SP. 2020. Diversity of flowers in Bantul as a local potential based on biology learning source. J Bioeducation 7 (2): 56-65. DOI: 10.29406/.v7i2.2134.

Panero JL, Crozier BS. 2016. Macroevolutionary dynamics in the early diversification of Asteraceae. Mol Phylogen Evol 99 (12): 116-132. DOI: 10.1016/j.ympev.2016.03.007.

Paniagua-Ibáñez M, López-Caamal A, Mussali-Galante P, Sánchez-Salinas E, Ortiz-Hernández ML, Ramírez-Rodríguez R, Tovar-Sánchez E. 2015. Morphological variation of *Cosmos bipinnatus* (Asteraceae) and its relation to abiotic variables in central Mexico. Rev Chil de Hist Nat 88 (14): 1-13. DOI: 10.1186/S40693-015-0044-4.

Perveen A, Khan M, Mansuri S, Tabassum T. 2016. Morphological studies on trichome of family Asteraceae. Intl J Biol Biotechnol 13 (2): 177-182.

Perwitasari DAG, Sindiya V, Mukarramah L, Rohimah S, Su'udi M. 2019. Barcode study of *Dendrobium* drug orchid based on *matK, rbcL,* and ITS gene sequences. Bioma 15 (1): 32-44. DOI: 10.21009/Bioma15(1).5.

Phong HX, Viet NT, Quyen NTN, Thinh PV, Trung NM, Ngan TTK. 2022. Phytochemical screening, total phenolic, flavonoid contents, and antioxidant activities of four spices commonly used in Vietnamese traditional medicine. Mater Today Proc 56 (3): A1-A5. DOI: 10.1016/j.matpr.2021.12.142.

POWO. 2022. Asteraceae Bercht. & J.Presl. https://powo.science.kew.org/taxon/urn:lsid:ipni.org:names: 319342-2. [28 July 2022]

Priska M, Peni N, Carvallo L, Ngapa YD. 2018. Review: Anthocyanins and their uses. Cakra Kimia 6 (2): 79-97. [Indonesian]

Purnobasuki H, Purnama PR, Kobayashi K. 2017. Morphology of four root types and anatomy of root-root junction in relation gas pathway of *Avicennia marina* (Forsk) Vierh roots. Vegetos 30 (2): 100-104. DOI: 10.5958/2229-4473.2017.00143.4.

Rahman AHM. 2013. Systematic studies on Asteraceae in the northern region of Bangladesh. Am J Life Sci 1 (4): 155-164. DOI: 10.11648/j.ajls.20130104.13.

Rahman AHM, Islam AKM, Rahman M. 2013. An anatomical investigation on Asteraceae family at Rajshahi Division, Bangladesh. Intl J Biosci 3 (1): 13-23. DOI: 10.11648/j.plant.20130102.11.

Rivera P, Terrazas T, Rojas-Leal A, Villasenor JL. 2019. Leaf architecture and anatomy of Asteraceae species in a xerophytic scrub in Mexico City, Mexico. Acta Bot Mex 126: e1515. DOI: 10.21829/abm126.2019.1515.

Rohimah S, Mukarramah L, Sindiya V, Veren Yuliana S, Gita Ayu K, Suudi M. 2018. Exploration of species and potential DNA barcode of *Thrixspermum* orchid in silico. J Biodjati 3 (2): 148-156. DOI: 10.1088/1755-1315/743/1/012092. [Indonesian]

Rozen S, Skaletsky H. 2000. Primer3 on the WWW for general users and for biologist programmers. In: Misener S, Krawetz SA (eds). Bioinformatics Methods and Protocols. Methods in Molecular Biology™. 132. Humana Press, Totowa.

Saarela JM, Sokoloff PC, Gillespie LJ, Consaul LL, Bull RD. 2013. DNA barcoding the Canadian Arctic Flora: Core plastid barcodes (rbcL + matK) for 490 vascular plant species. PLoS ONE 8 (10): e77982. DOI: 10.1371/journal.pone.0077982.

Safita G, Sakti ERE, Syafnir L. 2015. Antibacterial activity test of kenikir (*Cosmos caudatus* Kunth.) and sintrong (*Crassocephalum crepidioides* (Benth.) S.Moore) leaves against *Staphylococcus aereus* and *Pseudomonas aeruginosa* bacteria. Pros Penelitian Sivitas Akademika Unisba (Kesehatan dan Farmasi) 1 (20): 421-428. [Indonesian]

Saleh I, Trisnaningsih U, Dwirayani D, Syahadat RM, Atmaja ISW. 2020. Analysis of consumer preferences for two species of kenikir: *Cosmos caudatus* and *Cosmos sulphureus*. Mahatani 3 (1): 195-204. DOI: 10.52434/mja.v3i1.916. [Indonesian]

Santos RF, Nunes BM, Sá RD, Soares LAL, Randau KP. 2016. Morpho-anatomical study of *Ageratum conyzoides*. Rev Bras Farmacogn 26 (6): 679-687. DOI: 10.1016/j.bjp.2016.07.002.

Sanyal G, Mahadani AK, Mahadani P, Bhattacharjee P. 2015. Insertion-deletion as informative characters in DNA barcoding. Intl J Multimedia Ubiquitous Eng 10 (10): 67-74. DOI: 10.14257/ijmue.2015.10.10.07.

Sari DP, Harlita. 2018. Hand free section preparation trough replica technique for stomata identification. Proc Biol Educ Conf 15 (1): 660-664. [Indonesian]

Sari WDP, Suriani C, Handayani D. 2021. Glandular trichome in the Asteraceae family. BioLink Jurnal Biologi Lingkungan Industri dan Kesehatan 9 (2): 164-171.

Sass C, Little DP, Stevenson DW, Specht CD. 2007. DNA barcoding in the Cycadales: Testing the potential of proposed barcoding markers for species identification of cycads. PLoS ONE 2 (11**)**: e1154. DOI: 10.1371/journal.pone.0001154.

Sekar M, Abdullah MZB, Azian AY, SNasir SNB, Zakaria ZB, Abdullah MSB. 2014. Ten commonly available medicinal plants in Malaysia used for the treatment of diabetes – A review. Asian J Pharm Clin Res 7 (1): 1-5.

Schilling EE. 2006 *Helianthus*. In: Flora of North America Editorial Committee (eds). Flora of North America North of Mexico. Oxford University Press, New York.

Shaheen S, Jaffer M, Khan F, Hussain K, Hanif U, Younis S, Ilyas S, Ishtiaq S. 2018. Morpho-palynological assessment of medicinal flora of district Lahore, Pakistan based on LM and SEM. Microsc Res Tech 81 (12): 1397-1405. DOI: 10.1002/jemt.23096.

Smith DR, Burki F, Yamada T, Grimwood J, Grigoriev IV, Van Etten JL, Keeling PJ. 2011. The GC-rich mitochondrial and plastid genomes of the green alga *Coccomyxa* give insight into the evolution of organelle DNA nucleotide landscape. PLoS ONE 6 (8): e23624. DOI: 10.1371/journal.pone.0023624.

Sogandi. 2018. Molecular Biology for Molecular Identification of Bacteria. Universitas 17 Agustus 1945, Jakarta. [Indonesian]

Srilakshmi P, Naidu KC. 2014. A Study on foliar epidermal features in *Artemisia*, *Chrysanthemum* and *Cosmos* of the family Asteraceae. Intl J Adv Pharm Biol Chem 3 (1): 164-166.

Stace CA. 1984. The taxonomic importance of leaf surface. In: Heywood VH, Moore DM (eds). Current Concepts in Plant Taxonomy. Academic Press, London.

Susetyarini E, Wahyono P, Latifa R, Nurrohman E. 2019. The Identification of morphological and anatomical structures of *Pluchea indica*. J Phys Conf Ser 1539: 012001. DOI: 10.1088/1742-6596/1539/1/012001.

Syah AS, Sulaeman SM, Pitopang R. 2014. Asteraceae plant species at Mataue, Lore Lindu National Park. Online J Nat Sci 3 (3): 297-312. [Indonesian]

Tahir MA, Sarwar R, Safeer S, Hamza I, Khan MF. 2017. Anatomical variations in stomatal attributes of selected species of family Asteraceae. Commun Plant Sci 7 (2017002): 10-14. DOI: 10.26814/cps2017002.

Takada S, Iida H. 2014. Specification of epidermal cell fate in plant shoots. Front in Plant Sci 5: 49. DOI: 10.3389/fpls.2014.00049.

Tindi M, Mamangkey NGF, Wullur S. 2017. The DNA barcode and molecular phylogenetic analysis several bivalve species from North Sulawesi waters based on COI gene. Jurnal Pesisir dan Laut Tropis 1 (2): 33-38. DOI: 10.35800/jplt.5.2.2017.15050. [Indonesian]

Utami P. 2008. Medicinal Plant Smart Book. Agromedia Pustaka, Jakarta. [Indonesian]

Uzbek UH, Shahidan WNS. 2019. Tasty herb that heals: A review of *Cosmos caudatus* (Ulam Raja) and its potential uses in dentistry. World J Dent 10 (4): 321-324. DOI: 10.5005/jp-journals-10015-1651.

van den Bergh MH. 1994. *Cosmos caudatus* Kunth. In: Siemonsma JS, Piluek K. (eds). PROSEA 8. Vegetables. Prosea, Bogor.

Wahyuni DK, Rahayu S, Purnama PR, Saputro TB, Suharyanto, Wijayanti N, Purnobasuki H. 2019. Morpho-anatomical structure and DNA barcode of *Sonchus arvensis* L. Biodiversitas 20 (8): 2417-2426. DOI: 10.13057/biodiv/d200841.

Widyawati AT, Zulchi T. 2019. Efforts to develop the potential of minor vegetables. Pros Sem Nas Masy Biodiv Indon 5 (1): 117-122. DOI: 10.13057/psnmbi/m050122.

Willis KJ. 2017. State of the World's Plants 2017: Report. Royal Botanic Gardens, London.

Yu J, Wu X, Liu C, Newmaster S, Ragupathy S, Kress WJ. 2021. Progress in the use of DNA barcodes in the identification and classification of medicinal plants. Ecotoxicol Environ Saf 208: 111691. DOI: 10.1016/j.ecoenv.2020.111691.

Yusoff NAH, Bustamam MSA, Abas F, Khatib A, Rukayadi Y. 2014. Antimicrobial activity of *Cosmos caudatus* extract against foodborne pathogens. J Pure Appl Microbiol 8 (5): 3681-3688.

Yusoff NAH, Rukayadi Y, Abas F, Khatib A, Hassan M. 2021. Antimicrobial stability of *Cosmos caudatus* extract at varies pH and temperature, and compounds identification for application as food sanitiser. Food Res 5 (3): 83-91. DOI: 10.26656/fr.2017.5(3).710.